NANO LETTERS

Letter

Atomic Hole Doping of Graphene

Isabella Gierz, Christian Riedl, Ulrich Starke, Christian R. Ast, and Klaus Kern

Nano Lett., **2008**, 8 (12), 4603-4607 • DOI: 10.1021/nl802996s • Publication Date (Web): 16 November 2008

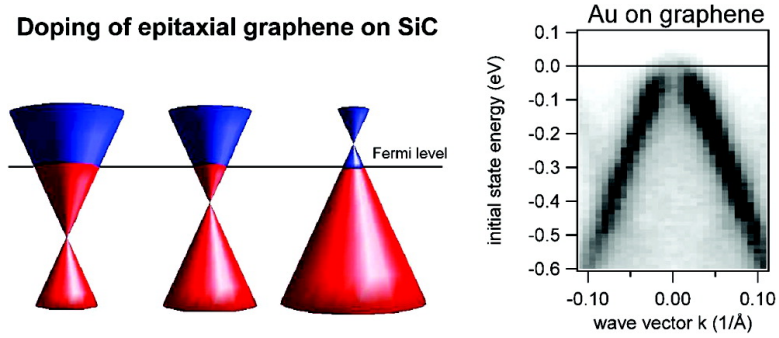

More About This Article

Additional resources and features associated with this article are available within the HTML version:

- Supporting Information
- Access to high resolution figures
- Links to articles and content related to this article
- Copyright permission to reproduce figures and/or text from this article

View the Full Text HTML

NANO LETTERS

2008
Vol. 8, No. 12
4603-4607

Atomic Hole Doping of Graphene

Isabella Gierz,[†] Christian Riedl,[†] Ulrich Starke,[†] Christian R. Ast,[*,†] and Klaus Kern[†,‡]

Max-Planck-Institut für Festkörperforschung, D-70569 Stuttgart, Germany, and Institut de Physique des Nanostructures, Ecole Polytechnique Fédérale de Lausanne, CH-1015 Lausanne, Switzerland

Received October 2, 2008; Revised Manuscript Received November 5, 2008

ABSTRACT

The application of graphene in nanoscale electronic devices requires the deliberate control of the density and character of its charge carriers. We show by angle-resolved photoemission spectroscopy that substantial hole doping in the conical band structure of epitaxial graphene monolayers can be achieved by the adsorption of bismuth, antimony, or gold. In the case of gold doping the Dirac point is shifted into the unoccupied states. Atomic doping presents excellent perspectives for large scale production.

Graphene is an excellent candidate for the next generation of electronic materials due to the strict two-dimensionality of its electronic structure as well as an extremely high carrier mobility.[1−3] A prerequisite for the development of graphene-based electronics is the reliable control of the type and density of the charge carriers by external (gate) and internal (doping) means. While gating has been successfully demonstrated for graphene flakes[1,4,5] and epitaxial graphene on silicon carbide,[6,7] the development of reliable chemical doping methods turns out to be a real challenge. In particular hole doping is an unsolved issue. So far it has only been achieved with reactive molecular adsorbates, which might be difficult to implement in device technology. Here we show by ultraviolet angle-resolved photoemission spectroscopy (ARUPS) that atomic doping of an epitaxial graphene layer on a silicon carbide substrate with bismuth, antimony, or gold presents effective means of p-type doping. Not only is the atomic doping the method of choice for the internal control of the carrier density. In combination with the intrinsic n-type character of epitaxial graphene on SiC, the charge carriers can be tuned from electrons to holes, without affecting the conical band structure.

The electronic structure of epitaxial graphene is two-dimensional by nature. It is a zero-gap semiconductor, i.e., a semimetal, with a conically shaped valence and conduction band reminiscent of relativistic Dirac cones for massless particles.[8,9] As this kind of band structure provides great potential for electronic devices, one of the key questions is how to dope the electronic structure with electrons or holes appropriately for the different devices (see Figure 1). The semimetallic character induced by the close proximity of valence and conduction band as well as the conical shape of the bands results from a delicate balance between the electrons and the lattice. The challenge here is to interact with the system just enough to add or remove electrons but not too much so as to modify or even collapse the electronic structure. Therefore, it is not an option to replace atoms

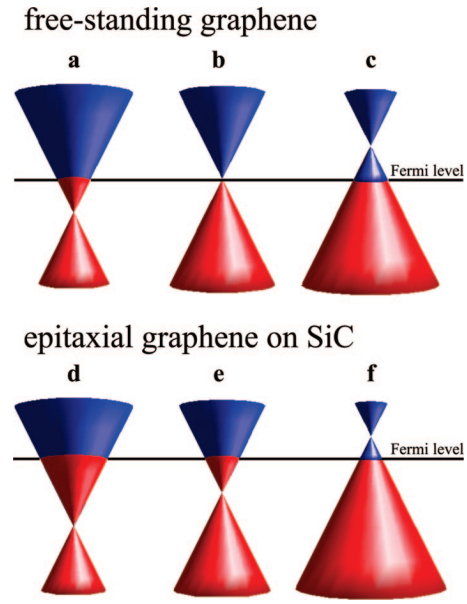

Figure 1. Doping graphene. Position of the Dirac point and the Fermi level of pristine and epitaxial graphene as a function of doping. The upper and lower panels show a free-standing graphene layer and an epitaxial graphene layer on silicon carbide, respectively. The left and right panels visualize n-type and p-type doping, respectively, while the center panels show the pure graphene layers. For the epitaxial graphene, a natural substrate induced n-type doping is present.

* Corresponding author, c.ast@fkf.mpg.de.
† Max-Planck-Institut für Festkörperforschung.
‡ Institut de Physique des Nanostructures, Ecole Polytechnique Fédérale de Lausanne.

10.1021/nl802996s CCC: $40.75
Published on Web 11/16/2008

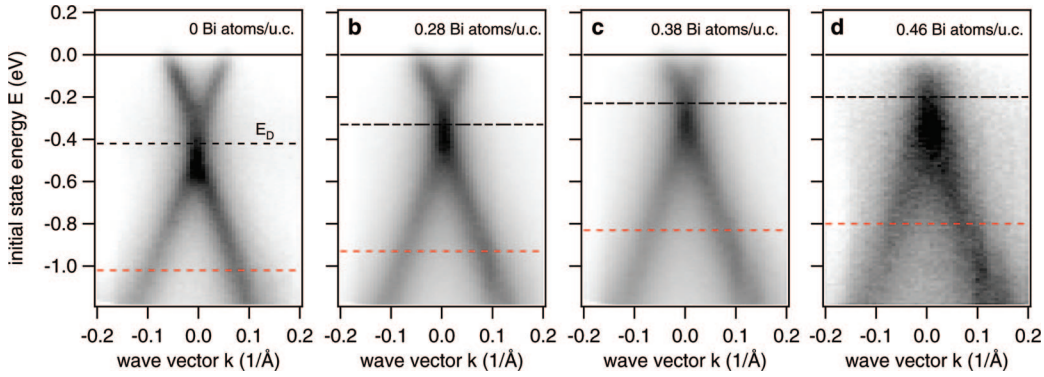

Figure 2. Doping graphene with Bi atoms. Experimental band structure of epitaxial graphene doped with bismuth atoms. (a) pristine graphene layer, (b)-(d) increasing amounts of bismuth atoms have been deposited.

within the graphene layer, as is common practice when doping silicon.

For graphene the doping is usually realized by adsorbing atoms and/or molecules on its surface, i.e., surface transfer doping.[10−13] For n-type (p-type) doping the electrons have to be released into (extracted out of) the graphene layer. A schematic sketch that compares the doping behavior of free-standing graphene with that of epitaxial graphene on SiC is displayed in Figure 1. The most significant difference between free-standing and epitaxial graphene on SiC is that epitaxial graphene is naturally n-doped due to charge transfer from the substrate (see Figure 1, panels b and e).

As alkali atoms easily release their valence electron, they very effectively induce n-type doping[14,15] (see Figure 1, panels a and d). In the case of epitaxial graphene, the Dirac point, where the apexes of the two conically shaped bands meet, is shifted further into the occupied states away from the Fermi level. However, aside from the fact that epitaxial graphene on silicon carbide is naturally n-doped, alkali atoms are very reactive and their suitability in electronic devices is more than questionable.

P-type doping for graphene (see Figure 1, panels c and f) is quite a bit more challenging. Many of the elements with a high electronegativity—e.g., nitrogen, oxygen, or fluorine—form strong dimer bonds. They would not likely form a stable adlayer on the graphene surface. Therefore, different molecules such as NO_2, H_2O, NH_3, or the charge transfer complex tetrafluorotetracyanoquinodimethane (F4-TCNQ) have been used to induce p-type doping in graphene.[16−19] However, NO_2, H_2O, and NH_3 are very reactive chemicals and therefore not suitable for use in an electronic material. F4-TCNQ on the other hand plays an important role in optimizing the performance in organic light-emitting diodes,[20,21] but would be incompatible with high-temperature processes. A viable alternative is presented by the heavier elements, which are not as reactive as, e.g., oxygen or fluorine. Although not obvious, because their electron affinity is somewhat lower than that of atomic carbon, bismuth as well as antimony turns out to be able to extract electrons out of the graphene sheet.

We have studied the valence band structure of a precisely prepared graphene monolayer[22] on 4H-SiC(0001) using ARUPS. Figure 2 shows the experimental band structure of epitaxial graphene doped with successively higher amounts of Bi atoms. The initial state energy E of the bands is plotted as a function of the electron wave vector k.[23] The intensity scale is linear with light and dark areas corresponding to low and high photoelectron current, respectively. The Dirac point is located at the $\bar{K}$-point, which lies in the corner of the hexagonal Brillouin zone. Figure 2a shows the pristine graphene layer. The linear dispersion of the valence and conduction bands is clearly visible. Due to the charge transfer with the SiC substrate, the Dirac cone of the conduction band is partially filled shifting the Dirac point into the occupied states by about 420 meV.[14,22,24] Panels b−d of Figure 2 display the evolution of the band structure when successively higher amounts of bismuth atoms per graphene unit cell (u.c.) as indicated in each panel are deposited on the graphene layer.[25] As the bismuth coverage increases, the Dirac point clearly shifts toward the Fermi level. Otherwise, the band structure remains unaltered by the bismuth adatoms; i.e., the linear dispersion is preserved. With increasing Bi coverage, the number of free charge carriers decreases as a successively smaller cross section of the conduction band intersects the Fermi level.

At higher bismuth coverage, the line width of the bands as well as the background increases. This is shown in more detail in Figure 3. The graph shows momentum distribution curves for different Bi coverages at an energy of 600 meV below the Dirac point (see dashed lines in Figure 2). The full widths at half-maximum (FWHM) are given on the right side and they indicate that the line width increases with increasing Bi coverages. This is in contrast to what has been found in refs 14 and 26 according to which we would expect that a decrease in carrier density leads to a decrease in line width. We conclude therefore, that this increase in line width is probably related to the fact that Bi atoms do not form an ordered structure but rather tend to form clusters on the surface, which leads to broadening of the photoemission features.

Very similar results have been obtained for antimony atoms deposited on the graphene layer. Antimony is also located in group V of the periodic table just above bismuth, so that a very similar doping behavior is expected. The experimental band structure is not shown here but looks very much like the data obtained for bismuth on graphene except

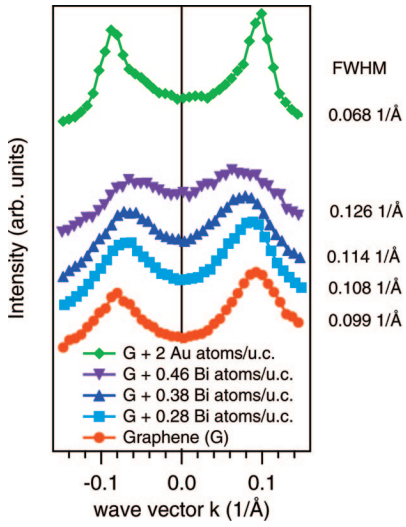

Figure 3. Line widths. Momentum distribution curves for graphene and different adatom quantities. The cuts were taken 600 meV below the Dirac point (see dashed red lines in Figures 2 and 5). The FWHM for the corresponding spectra are given at the right of the panel. The spectra have been shifted with respect to each other.

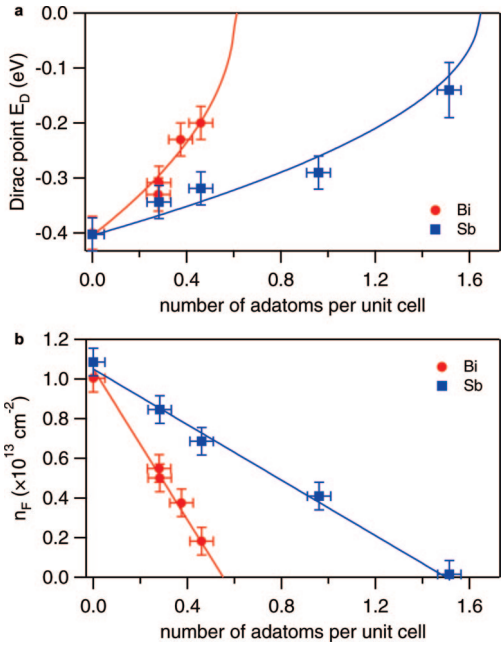

Figure 4. Doping parameters of Bi and Sb: (a) position of the Dirac point E_D and (b) free charge carrier density n_F as a function of doping with bismuth atoms (red circles) and antimony atoms (blue squares) (adatoms per graphene unit cell). The solid lines represent a simple model calculation assuming an electron transfer of 0.01 and 0.0036 electrons per Bi and Sb atom, respectively.

that it takes a higher antimony coverage to reach the same doping level.

A more quantitative analysis of the bismuth and antimony doping is displayed in Figure 4. Panel a shows the evolution of the Dirac point as a function of the coverage, which is given in number of atoms per graphene unit cell. The Dirac point clearly approaches the Fermi level with increasing doping indicating that there is charge transfer from the graphene layer to the adatoms. A simple theoretical model

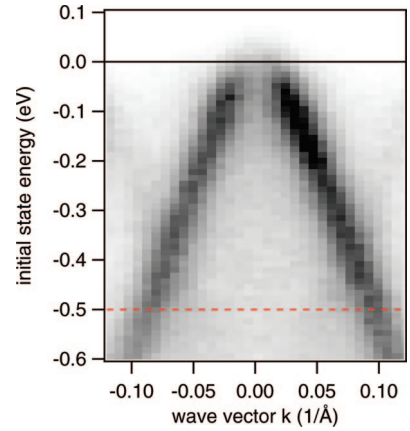

Figure 5. Hole doping with Au. Experimental band structure of Au atoms on epitaxial graphene. The bands are well-defined with the Dirac point at about 100 meV above the Fermi level and a charge carrier density for the holes of about 5×10^{11} cm^{-2}.

based on the linear density of states for the graphene layer has been used to estimate the doping effect of the bismuth atoms assuming that the charge transfer is proportional to the amount of dopant atoms

$$E_D = -\sqrt{\pi}\hbar v_F \sqrt{N_0 - N_h} \quad (1)$$

Here E_D is the Dirac point, with the zero of the energy scale referenced to the Fermi level. The Fermi velocity $\hbar v_F = 6.73$ eV Å was determined experimentally from the slope of the linear band structure for monolayer graphene and agrees well with values given in literature,[3,14] N_0 is the number of electrons in the conduction band for zero doping, and N_h is the number of holes doped into the graphene layer. Using eq 1, we find from the data that about 0.01 electrons per bismuth atom and 0.0036 electrons per antimony atom are extracted from the graphene layer. The Dirac point follows the respective solid lines plotted in Figure 4a. It would reach the Fermi level for a coverage of 0.61 bismuth atoms and 1.65 antimony atoms per unit cell. The experiment shows, however, that for higher coverages the bands become broader and less well-defined. At this point the average distance between adatoms approaches the one of monolayer coverage which makes a cluster formation of the Bi atoms very likely, so that the photoelectrons will interact and scatter in the Bi clusters.

In Figure 4b, the free charge carrier density n_F of the graphene layer is plotted as a function of adatoms per unit cell. n_F is proportional to the area enclosed by the Fermi surface and therefore can be extracted from the experimental data through the Fermi wave vector k_F. Here we assume a circular Fermi surface with an area of πk_F^2 and take into account that the density of states in momentum space is constant. Including the spin and valley degeneracy the free charge carrier density is given by $n_F = k_F^2/\pi$. The charge carrier density is clearly reduced as the number of adatoms increases, indicating hole doping. The solid line shows a linear dependence of the charge carrier density as a function of bismuth coverage with a very good correspondence to the experimental data assuming the same values for the electron transfer per adatom as above.

For actual p-type doping with holes as charge carriers, the Dirac point has to shift into the unoccupied states. A

further increase of the electron transfer from the graphene layer to the adatoms is desirable. The natural starting point would be an element with a higher electron affinity than bismuth or antimony. Motivated by this, we have deposited gold atoms on epitaxial graphene, as its electron affinity is about twice as high as that for bismuth and as recent phototransport experiments indicated that gold contacts induce p-doping in graphene.[27] The experimental band structure for about two gold atoms per graphene unit cell shown in Figure 5 clearly displays p-type doping. Both branches of the valence band cone clearly cross the Fermi level close to the $\bar{K}$-point leaving the valence band partially unoccupied. By extrapolating the linear band structure into the unoccupied states, we estimate the Dirac point to be about 100 meV above the Fermi level and a free charge carrier density of the holes of about 5×10^{11} cm^{-2}. This means that the Dirac point is shifted by about 520 meV compared to the pristine graphene layer.

We can compare these experimental findings with theoretical calculations in the literature for graphene on metal contacts[28] as well as metal adlayers on graphene.[29] Qualitatively the results compare very well as for both the adlayer as well as the metal contact hole doping is predicted. Quantitatively, the predicted Fermi level shift for the metal contact[28] is with only about 200 meV less than half of the experimental value. The reason for this could be that the doping properties from the bulk are less effective than those from an adlayer. The work function shift which is calculated for the adlayer in ref 29 cannot be compared to the experimental data, because both the position of the Fermi level and the core level shift are influenced by a number of different contributions, such as charge transfer or the local chemical environment.

The bands in Figure 5 are much narrower than those for the bismuth adatoms in Figure 2d even though the gold coverage is much higher than the bismuth coverage. This can be seen in the momentum distribution curve in Figure 3. The line width decreases substantially by about 30% compared to the clean graphene layer. The sharp band structure suggests on the one hand that gold forms an ordered and/or smoother structure with the graphene layer but also that the scattering rate is decreased based on a lower charge carrier density according to refs 14 and 26. Furthermore, the p-type doping in Figure 5 is only induced after a post-annealing of the sample to at least 700 °C. Similar to what has been observed for gold atoms binding to pentacene,[30] an actual bond between the gold atom and the graphene is formed after a certain activation barrier is overcome. The chemical bond formation is supported by X-ray photoelectron spectroscopy results, showing a clear splitting of the C 1s core level after annealing the sample at 700 °C, which is not present for the clean graphene layer. Interestingly, while this goes beyond the idea of surface transfer doping, where a covalent bond between adatom and graphene layer is not present, the peculiar band structure of graphene with its linear dispersion remains intact. This clearly demonstrates that for a coverage of about two gold atoms per graphene unit cell the Dirac point can be shifted above the Fermi level leaving the valence band partially unoccupied. Surprisingly, the estimated electron transfer is only 0.0024 electrons per gold atom, which is only a quarter of the value found for bismuth, where, however, no chemical bond to the graphene layer is formed.

Our results demonstrate that p-type doping of an epitaxial graphene layer is possible by means of simple atoms. While bismuth and antimony were only able to shift the Dirac point in the direction of the Fermi level, i.e., reduce the natural n-type doping of the substrate, gold actually shifted the Dirac point into the unoccupied states thereby inducing p-type doping. Epitaxial graphene on silicon carbide becomes a feasible alternative to conventional electronic materials as n-type doping is naturally induced and p-type doping can be achieved by doping with gold atoms, which are easily processed. With its potential for large scale production[6] all the advantages of epitaxial graphene, e.g., the strict two-dimensionality, high carrier mobility, high current densities, and ballistic transport at room temperature,[3] are available for device application.

Supporting Information Available: Details of sample preparation and photoemission experiments. This material is available free of charge via the Internet at http://pubs.acs.org.

References

(1) Novoselov, K. S.; Geim, A. K.; Morozov, S. V.; Jiang, D.; Zhang, Y.; Dubonos, S. V.; Grigorieva, I. V.; Firsov, A. A. *Science* **2004**, *306*, 666.
(2) de Heer, W. A.; Berger, C.; Wu, X.; First, P. N.; Conrad, E. H.; Li, X.; Li, T.; Sprinkle, M.; Hass, J.; Sadowski, M. L.; Potemski, M.; Martinez, G. *Solid State Commun.* **2007**, *143*, 92.
(3) Geim, A. K.; Novoselov, K. S. *Nat. Mater.* **2007**, *6*, 183.
(4) Oostinga, J. B.; Heersche, H. B.; Liu, X.; Morpurgo, A. F.; Vandersypen, L. M. K. *Nat. Mater.* **2008**, *7*, 151.
(5) Zhang, Y.; Tan, Y.-W.; Stormer, H. L.; Kim, P. *Nature* **2005**, *438*, 201.
(6) Kedzierski, J.; Hsu, P.-L.; Healey, P.; Wyatt, P. W.; Keast, C. L.; Sprinkle, M.; Berger, C.; de Heer, W. A. *IEEE Trans. Electron Devices* **2008**, *55*, 2078.
(7) Gu, G.; Nie, S.; Feenstra, W. J.; Devaty, R. P.; Choyke, W. J. *Appl. Phys. Lett.* **2007**, *90*, 253507.
(8) Wallace, P. R. *Phys. Rev.* **1947**, *71*, 622.
(9) Slonczewski, J. C.; Weiss, P. R. *Phys. Rev.* **1958**, *109*, 272.
(10) Maier, F.; Riedel, B.; Mantel, J.; Ristein, J. *Phys. Rev. Lett.* **2000**, *85*, 3472.
(11) Chakrapani, V.; Angus, J. C.; Anderson, A. B.; Wolter, S. D.; Stoner, B. R.; Sumanasekera, G. U. *Science* **2007**, *318*, 1424.
(12) Ristein, J. *Science* **2006**, *313*, 1057.
(13) Sque, S. J.; Jones, R.; Briddon, P. R. *Phys. Status Solidi A* **2007**, *204*, 3078.
(14) Bostwick, A.; Ohta, T.; Seyller, T.; Horn, K.; Rotenberg, E. *Nat. Phys.* **2007**, *3*, 36.
(15) Ohta, T.; Bostwick, A.; Seyller, T.; Horn, K.; Rotenberg, E. *Science* **2006**, *313*, 951.
(16) Chen, W.; Chen, S.; Qui, D. C.; Gao, X. Y.; Wee, A. T. S. *J. Am. Chem. Soc.* **2007**, *129*, 10419.
(17) Hwang, E. H.; Adam, S.; Das Sarma, S. *Phys. Rev. B* **2007**, *76*, 195421.
(18) Wehling, T. O.; Novoselov, K. S.; Morozov, S. V.; Vdovin, E. E.; Katsnelson, M. I.; Geim, A. K.; Lichtenstein, A. I. *Nano Lett.* **2008**, *8*, 173.
(19) Zhou, S. Y.; Siegel, D. A.; Fedorov, A. V.; Lanzara, A. *Phys. Rev. Lett.* **2008**, *101*, 086402.
(20) Blochwitz, J.; Pfeiffer, M.; Fritz, T.; Leo, K. *Appl. Phys. Lett.* **1998**, *73*, 729.
(21) Zhou, X.; Pfeiffer, M.; Blochwitz, J.; Werner, A.; Nollau, A.; Fritz, T.; Leo, K. *Appl. Phys. Lett.* **2001**, *78*, 410.
(22) Riedl, C.; Zakharov, A. A.; Starke, U. *Appl. Phys. Lett.* **2008**, *93*, 033106.

(23) The measurements were taken at the $\overline{K}$-point with the wave vector axis perpendicular to the $\overline{\Gamma K}$-high symmetry line.
(24) Zhou, S. Y.; Gweon, G.-H.; Fedorov, A. V.; First, P. N.; de Heer, W. A.; Lee, D.-H.; Guinea, F.; Castro Neto, A. H.; Lanzara, A. *Nat. Mater.* **2007**, *6*, 770.
(25) The graphene unit cell used here has a lattice constant of 2.46 Å (hexagonal lattice) and contains two graphene atoms.
(26) Hwang, E. H.; Yu-Kuang Hu, B.; Das Sarma, S. *Phys. Rev. B* **2007**, *76*, 115434.
(27) Lee, E. J. H.; Balasubramanian, K.; Weitz, R. T.; Burghard, M.; Kern, K. *Nat. Nanotechnol.* **2008**, *3*, 486.
(28) Giovanetti, G.; Khomyakov, P. A.; Brocks, G.; Karpan, V. M.; van der Brink, J.; Kelly, P. J. *Phys. Rev. Lett.* **2008**, *101*, 026803.
(29) Chan, K. T.; Neaton, J. B.; Cohen, M. L. *Phys. Rev. B* **2008**, *77*, 235430.
(30) Repp, J.; Meyer, G.; Paavilainen, S.; Olsson, F. E.; Persson, M. *Science* **2006**, *312*, 1196.

NL802996S